Available online at www.sciencedirect.com
ScienceDirect
The International Journal of Biochemistry & Cell Biology 39 (2007) 2324–2338
IJBCB
www.elsevier.com/locate/biocel

Overexpression of MMP9 in macrophages attenuates pulmonary fibrosis induced by bleomycin☆

Sandra Cabrera[a], Miguel Gaxiola[b], José Luis Arreola[b], Remedios Ramírez[a], Paul Jara[a], Jeanine D'Armiento[c], Thomas Richards[d], Moisés Selman[b], Annie Pardo[a,*]

[a] *Facultad de Ciencias, Universidad Nacional Autónoma de México, Mexico*
[b] *Instituto Nacional de Enfermedades Respiratorias, Mexico*
[c] *Department of Medicine, Columbia University, New York, NY, USA*
[d] *University of Pittsburgh Medical Center, Pittsburgh, PA, USA*

Received 18 March 2007; received in revised form 17 June 2007; accepted 23 June 2007
Available online 12 July 2007

Abstract

Pulmonary fibrosis is a common response to a variety of lung injuries, characterized by fibroblast/myofibroblast expansion and abnormal accumulation of extracellular matrix. An increased expression of matrix metalloprotease 9 (MMP9) in human and experimental lung fibrosis has been documented, but its role in the fibrotic response is unclear. We studied the effect of MMP9 overexpression in bleomycin-driven lung fibrosis using transgenic mice expressing human MMP9 in alveolar macrophages (hMMP9-TG). At 8 weeks post-bleomycin, the extent of fibrotic lesions and OH-proline content were significantly decreased in the TG mice compared to the WT mice. The decreased fibrosis in hMMP9-TG mice was preceded by a significant reduction of neutrophils and lymphocytes in bronchoalveolar lavage (BAL) at 1 and 4 weeks post-bleomycin, respectively, as well as by significantly less TIMP-1 than the WT mice. From a variety of cytokines/chemokines investigated, we found that BAL levels of insulin-like growth factor binding protein-3 (IGFBP3) as well as the immunoreactive protein in the lungs were significantly lower in hMMP9-TG mice compared with WT mice despite similar levels of gene expression. Using IGFBP-3 substrate zymography we found that BAL from TG mice at 1 week after bleomycin cleaved IGFBP-3. Further, we demonstrated that MMP9 degraded IGFBP-3 into lower molecular mass fragments. These findings suggest that increased activity of MMP9 secreted by alveolar macrophages in the lung microenvironment may have an antifibrotic effect and provide a potential mechanism involving IGFBP3 degradation.

Keywords: MMPs; Lung fibrosis; IGFBP3; TIMPs

1. Introduction

Pulmonary fibrosis is the final consequence of a heterogeneous group of disorders known as interstitial lung diseases (Pardo & Selman, 2002). Lung fibrotic remodeling is characterized by fibroblast/myofibro-

☆ This work was submitted in partial fulfillment of the requirements to obtain the PhD degree for S.C. at Universidad Nacional Autonoma de Mexico.

* Corresponding author at: Facultad de Ciencias, UNAM, Apartado Postal 21-630, Coyoacan, Mexico DF, CP 04000, Mexico. Tel.: +52 55 5622 1536; fax: +52 55 5622 1503.
E-mail address: aps@fciencias.unam.mx (A. Pardo).

1357-2725/$ – see front matter © 2007 Elsevier Ltd. All rights reserved.
doi:10.1016/j.biocel.2007.06.022

blast activation and unbalanced extracellular matrix accumulation resulting in extensive structural disorganization of the lung. The irreversible changes in the lung architecture result in progressive organ dysfunction and usually a fatal outcome.

Several studies have shown that matrix metalloproteases (MMPs) play an important role in the pathogenesis of pulmonary fibrosis, and the presence of several of these proteases even in the advanced stages of fibrosis highlights the dynamic nature of scarring within the lung. However, the precise role of MMPs in the molecular mechanisms that characterize the fibrotic response is not completely understood (Pardo & Selman, 2006).

MMPs are a family of peptidases with multiple substrate affinities. They are not only collectively capable of cleaving all components of ECM but can also process bioactive mediators, such as growth factors, cytokines, chemokines, and cell-surface receptors (Nagase, Visse, & Murphy, 2006).

From the 23 members of the human MMPs family, MMP9 (gelatinase B), is one of the enzymes shown to be elevated in several human and experimental interstitial lung diseases (Fukuda, Ishizaki, Kudoh, Kitaichi, & Yamanaka, 1998; Hayashi et al., 1996; Pardo et al., 2000; Pérez-Ramos et al., 1999; Selman et al., 2000; Yaguchi, Fukuda, Ishizaki, & Yamanaka, 1998). In idiopathic pulmonary fibrosis (IPF) MMP9 is highly expressed in the lungs and BAL fluids and localized mainly to epithelial cells, neutrophils, and alveolar macrophages (Selman et al., 2000; Suga et al., 2000).

Experimental models of lung fibrosis, including those induced by paraquat plus hyperoxia, silica inhalation, or bleomycin instillation, have also exhibited an increase in MMP9 activity which has been associated with the disruption of the alveolar epithelial basement membrane (Cisneros-Lira, Gaxiola, Ramos, Selman, & Pardo, 2003; Pardo et al., 2003; Ruiz et al., 2003).

However, despite the putative profibrotic role of MMP9 in lung injury, MMP9 null mice develop similar fibrosis to wild-type littermates, after bleomycin instillation, although the lungs of the MMP9 deficient mice showed minimal alveolar bronchiolization (Betsuyaku, Fukuda, Parks, Shipley, & Senior, 2000).

In order to further understand the role of MMP9 in lung fibrosis, we have analyzed the effect of MMP9 overexpression in bleomycin driven lung fibrosis, using transgenic mice (TG) expressing human MMP9 in macrophages (hMMP9 TG), and following the model for 16 weeks. Our results indicate that hMMP9 TG mice develop reduced lung fibrosis compared to wild-type mice and suggest a possible mechanism related to insulin-like growth factor binding protein-3 cleavage by MMP9.

2. Methods

2.1. Generation of transgenic mice

Transgenic mice expressing human MMP9 were generated as follows. The 2.4 kb cDNA of human MMP9 (a gift from G. Goldberg, Washington University) was cloned into a vector containing the splice site and polyadenylation sequence of the β-globin gene, and placed under the control of the Scavenger Receptor A enhancer-promoter (SREP; a gift from Dr. Glass, UC, San Diego), a promoter that allows targeted expression of genes specifically in differentiated macrophages of transgenic mice (Lemaitre et al., 2001; Lemaitre, O'Byrne, Dalal, Tall, & D'Armiento, 1999). The final construct (8.3 kb) was removed with NcoI/XhoI digestion and purified by CsCl centrifugation. The construct was microinjected into fertilized mouse eggs (F1 [C57BL/6 × CBA] X F1[C57BL/6 × CBA]). Twelve live newborn mice were obtained of which three carried the transgene. One of the lines did not transmit to their progeny and the other two lines were established. Lines that expressed the transgene were established through Southern blot and PCR analysis, using specific primers for human MMP-9 (sense: 5′GCCAGGACCGCTTCTACTGGCGCGT3′; anti-sense: 5′ CAGAACAGAATACCAGTTTGTATC 3′) resulting in a 200 bp fragment.

2.2. Generation of the study population and bleomycin instillation

The mouse line selected for the study population expressed human MMP-9 within their peritoneal macrophages at levels comparable to cultured human macrophages, as determined by zymography. This line was crossed into a pure C57BL/6 background for six generations. Mice between 8 and 10 weeks of age were instilled intratracheally with 0.13 U/ 10 g of bleomycin (Blenoxane, Bristol-Myers Squibb Co.) in 50 μl sterile saline (Pardo et al., 2003). Control animals were treated with an equal volume of sterile saline. Mice were sacrificed at 1, 4, 8, 12 and 16 weeks after bleomycin or saline treatment. Mice were housed in specific pathogen-free conditions and provided with food and water *ad libitum*. All studies and procedures were approved by the Ethical Committee at the National Institute of Respiratory Diseases.

Table 1
Primers used for quantitative real-time PCR

Gene	Sense primer (5′ to 3′)	Reverse primer (5′ to 3′)	Amplicon length (bp)
MMP-9 (Human)	CCC TTC TAC GGC CAC TAC TGT	GCG ATG GCG TCG AAG ATG TT	75
MMP-9 (Mouse)	TGG CTT TTG TGA CAG GCA CTT	CCC GAC ACA CAG TAA GCA TTC	126
IGFBP-3	CGT CCA CAT CCC AAA CTG TG	CCA AGG GGA AAG ACG ACG TA	148
18S rRNA	GTA ACC CGT TGA ACC CCA TT	CCA TCC AAT CGG TAG TAG CG	140

2.3. RT-PCR and quantitative real-time PCR amplification

Total lung RNA was extracted from mouse lungs using TRIzol reagent (Invitrogen Life Technologies, Grand Island, NY) and reversed transcribed into cDNA (Advantage RT-for-PCR Kit; Clontech, Palo Alto, CA) according to the manufacturer's instructions. Primers used for the PCR are listed in Table 1. Quantitative real-time PCR amplification was performed using i-Cycler iQ Detection System (Bio-Rad, Hercules, CA) as previously described (Ruiz et al., 2003). The standard curve method was used to quantify the expression of the target genes and 18S rRNA in each sample. For each experimental sample, a gene was considered not to be expressed if amplification was not detected by cycle 40. The specificity of the PCR products was confirmed by melting curve analysis and gel electrophoresis. The normalized results were expressed as the ratio of the target gene to 18S rRNA.

2.4. Morphology

Lungs were lavaged with saline solution through the pulmonary artery, and the right lung was removed, fixed by inflation with 4% paraformaldehyde in phosphate-buffered saline (PBS) at continuous pressure of 25 cmH_2O and embedded in paraffin. Sections were stained with hematoxylin-eosin and Masson's trichrome stain, and were scored blindly for severity and extent of the lesions and percentage of fibrosis as previously described (Pardo et al., 2003).

2.5. Immunohistochemistry

The tissue sections were deparaffinized and were then rehydrated and blocked with 3% H_2O_2 in methanol followed by antigen retrieval in a microwave in 10 mM citrate buffer, pH 6.0. Tissue sections were treated with universal blocking solution (Biogenex, San Ramon, CA) for 10 min, and then incubated with anti-human MMP-9 antibody (2 μg/ml; Chemicon, CA) or anti-mouse IGFBP-3 antibody (2 μg/ml; R&D Systems, Inc, MN) overnight at 4 °C. A secondary biotinylated anti-immunoglobulin followed by horseradish peroxidase-conjugated streptavidin (BioGenex) was used according to the manufacturer's instructions. 3-Amino-9-ethyl-carbazole (BioGenex) in acetate buffer containing 0.05% H_2O_2 was used as substrate. The sections were counterstained with hematoxylin. The primary antibody was replaced by nonimmune serum for negative control slides.

2.6. Hydroxyproline assay

To quantify collagen deposition, left lungs were hydrolyzed in HCl 6N for 24 h at 110 °C, and hydroxyproline levels were quantified as previously described (Cisneros-Lira et al., 2003; Woessner, 1961). Each sample was tested in triplicate. Data are expressed as micrograms of hydroxyproline per left lung.

2.7. Bronchoalveolar lavage (BAL)

After semi-excision of the trachea, a 20-gauge intravenous catheter (Becton Dickinson, Franklin Lakes, NJ) was inserted into the trachea, and airspaces were lavaged twice with 0.6 ml of sterile saline. BAL was centrifuged at 1500 rpm for 10 min at 4 °C, and supernatant was stored at −80 °C for subsequent biochemical analyses. Cell counts were performed by manual counting under light microscopy with a standard hemocytometer. Differential cell counts were obtained using Wright-Giemsa stain.

2.8. Myeloperoxidase activity assay

Myeloperoxidase (MPO) activity was determined in lung tissue and BAL fluids. Lung tissues were homogenized in 50 mM potassium phosphate buffer solution (pH 6.0) with 5% hexadecyltrimethyl ammonium bromide (Sigma–Aldrich, St. Louis, MO, USA). The homogenate was sonicated and centrifuged at 12,000 × g for 15 min at 4 °C. Aliquots of the lung supernatants or BAL fluids were mixed with potassium phosphate buffer containing *o*-dianisidine-2HCl (0.167 mg/ml; Sigma–Aldrich)

and 0.0005% H_2O_2. After 15 min of incubation, 100 μl of 1% NaN3 was added to stop the reaction, and the optical density of the mixture was measured at 460 nm. Purified MPO (10 U/ml; Sigma–Aldrich) was used as a positive and internal control for assay accuracy. MPO activity was expressed as units/μg of protein.

2.9. Gelatin and IGFBP-3 substrate zymography

For gelatinolytic activity, lung tissue (20 mg/ml) and BAL macrophages were homogenized in 10 mM CHAPS (Sigma Chemical Co., St. Louis, MO), 20 mM HEPES pH 7.5 plus 150 mM NaCl. After centrifugation, supernatant aliquots containing 15 μg of protein, were analyzed in gelatin substrate SDS-PAGE as previously described (Pérez-Ramos et al., 1999). Alike gels were incubated in the presence of 20 mM EDTA.

For IGFBP-3, BAL aliquots were analyzed by 8.5% SDS-PAGE containing 2 mg/ml mouse IGFBP-3 (R&D Systems, Inc). After electrophoresis gels were washed in 2.5% Triton X-100 (Sigma, St. Louis, MO, USA) for 1 h and were then placed in the enzyme buffer (50 mM Tris–HCl, pH 8.0, 5 mM $CaCl_2$ and 5 mM $ZnCl_2$) overnight at 37 °C. Cleaved fragments of mIGFBP-3 were subjected to capillary transfer onto a polyvinylidene difluoride (PVDF) membrane (Invitrogene, Carlsbad CA) overnight at 37 °C, as described previously (Fowlkes, Enghild, Suzuki, & Nagase, 1994). Under these conditions, only proteolytic fragments of mIGFBP-3 transfer from the gel to the membrane. The membrane was incubated overnight with goat anti-mIGFBP-3 antibody (1 μg/ml; R&D Systems, Inc.) at 4 °C and then for 1 h with peroxidase-labeled secondary antibody (Zymed Laboratories, Inc., San Francisco, CA). Cleaved fragments mIGFBP-3 was visualized with ECL chemiluminescent reagent (Amersham Corp., Arlington Heights, IL).

2.10. Mouse cytokine antibody array

Mouse cytokine antibody arrays (RayBiotech, Inc., Norcross, GA) was used to quantify in BAL samples from either saline or bleomycin treated (1 and 4 weeks): interferon-gamma inducible protein 10 (IP-10), CXCL10, granulocyte-macrophage colony-stimulating factor (GM-CSF), insulin growth factor binding protein (IGFBP)-3 and -5, interleukin-1 beta (IL-1b), keratinocyte-derived chemokine (KC) platelet factor-4 (PF-4), stromal derived factor-1 (SDF-1), tissue inhibitor of metalloproteases-1 (TIMP-1), and tumor necrosis factor alpha (TNF-α). Relative cytokine levels were compared after densitometry analysis. Results were expressed as arbitrary units.

2.11. Proteolytic activity of MMP9 on IGFBP-3

Recombinant mouse IGFBP-3 (1 μg) was incubated with human MMP9 (kindly donated by Rafael Fridman, Wayne State University Detroit MI) in enzyme buffer (0.1 M glycine pH 8.0, 5 mM $CaCl_2$ and 5 mM $ZnCl_2$) overnight at 37 °C, alone or with amino phenyl mercuric acetate (APMA; 1.5 mM) used as MMP activator or EDTA (100 mM) used as MMP inhibitor. After electrophoresis in 15% SDS, gel was transferred to a PVDF membrane and immunoblotted with goat anti-mIGFBP-3 antibody. Intact rmIGFBP-3 and cleaved fragments were visualized with ECL chemiluminescent reagent (Amersham Corp., Arlington Heights, IL).

2.12. Statistical analysis

Differences between groups were analyzed by the Tukey's test. Additionally, linear regression with log-transformed hydroxyproline concentration as response variable was used to analyze effects of mice type and treatment. Likelihood ratio testing was used to compute p-values.

3. Results

3.1. Evidence of human MMP9 in transgenic mice

Levels of mouse and human MMP9 gene expression were assessed by quantitative real-time PCR in total RNA isolated from lungs of bleomycin or saline-treated mice. Mouse MMP9 mRNA was significantly increased at 1, 4 and 8 weeks after bleomycin as compared with saline-treated controls in both hMMP9 TG and WT mice ($p < 0.05$; Fig. 1A). No significant difference in the gene expression level was found between the TG and WT mice at any time point. Confirming the genotype of the hMMP9 TG mice, human MMP9 was expressed in the control lungs and the gene expression was significantly elevated at 1 and 4 weeks after bleomycin treatment ($p < 0.05$; Fig. 1B). By immunohistochemistry using a specific anti-human MMP9 antibody we found as expected that hMMP9 was expressed by interstitial and alveolar macrophages in lungs from hMMP9 TG mice as shown in a representative section of 4 weeks post-bleomycin (Fig. 1C, inset). Lung tissue gelatin zymography demonstrated

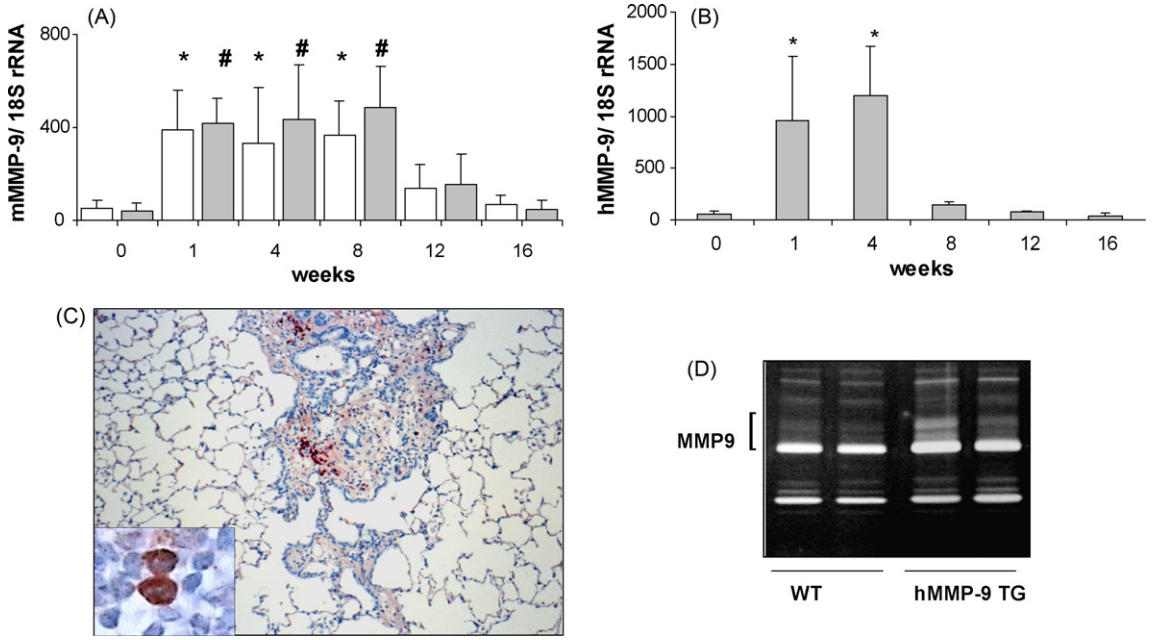

Fig. 1. Quantitative real-time PCR, gelatin zymography and immunolocalization of MMP9. Mouse (A) and human (B) MMP9 mRNA levels were determined by quantitative real-time PCR in lung tissue from WT (white bars) and hMMP-9 TG (gray bars), control and bleomycin-treated mice. Quantification of mRNA was performed by determining the threshold cycle; standard curves were constructed using the values obtained from serially diluted cDNA. Results were normalized for 18S rRNA and are shown as mean ± S.D. ($n = 6$). * and $^{\#}p < 0.05$ compared with their respective controls. (C) Immunolocalization of human MMP9 at 4 weeks post-bleomycin (original magnification 10×). Inset: hMMP9 immunoreactive macrophages (original magnification 40×). (D) Zymogram showing gelatinolytic activity in lung tissue from WT and hMMP-9 TG control mice.

MMP9 increased activity in the hMMP9 TG mice (Fig. 1D).

3.2. BAL inflammatory response

To evaluate the inflammatory response to bleomycin, total and differential cell counts were compared in BALF from hMMP9 TG and WT mice. Administration of bleomycin significantly increased the total number of inflammatory cells, at 1 and 4 weeks in both groups of mice ($p < 0.05$), without significant differences between WT and TG mice at any time point (Fig. 2A). However, analysis of the cell profile demonstrated that the inflammatory response was different. As shown in Fig. 2B, neutrophils were significantly increased in WT mice as compared to hMMP9 TG mice at 1 week after bleomycin ($3.7 \pm 0.7 \times 10^5$ versus $2.0 \pm 0.3 \times 10^5$; $p < 0.05$). Also, a significant increase in lymphocytes was observed in WT mice at 4 weeks after bleomycin compared to hMMP9 TG mice ($2.5 \pm 0.4 \times 10^5$ versus $1.3 \pm 0.3 \times 10^5$; $p < 0.05$); (Fig. 2C). There was no statistical difference in the number of macrophages, although as expected, BAL macrophages from TG mice exhibited increased MMP9 expression (Fig. 2D, inset).

3.3. Lung tissue and BAL myeloperoxidase activity

Neutrophil infiltration was quantified by measuring myeloperoxidase activity in lung tissue and BAL fluids. As shown in Fig. 3A, and B, MPO activity was significantly increased in lung tissue and BAL in both hMMP9 TG and WT mice at 1 week post-bleomycin administration, as compared to controls ($p < 0.05$). However, MPO activity in both lung tissue and BAL fluids was significantly higher in WT mice at 1 week post-bleomycin compared with hMMP9 TG mice ($p < 0.05$). Paralleling BAL neutrophil reduction, MPO activity decreased in both WT and hMMP9 TG at 4 weeks.

3.4. Semi-quantitative evaluation of lung histology

At 8–10 weeks of age (when animals were instilled), lung morphology of hMMP9 TG mice did not show differences compared with normal lungs of wild-type animals (Fig. 4A and D). However, with ageing (18–24 weeks) during the following-up of the experiment, the lungs of the majority of the TG mice exhibited some emphysematous-like lesions (data not shown). Seven days after bleomycin instillation, multifocal interstitial and intra-alveolar inflammation was observed in both

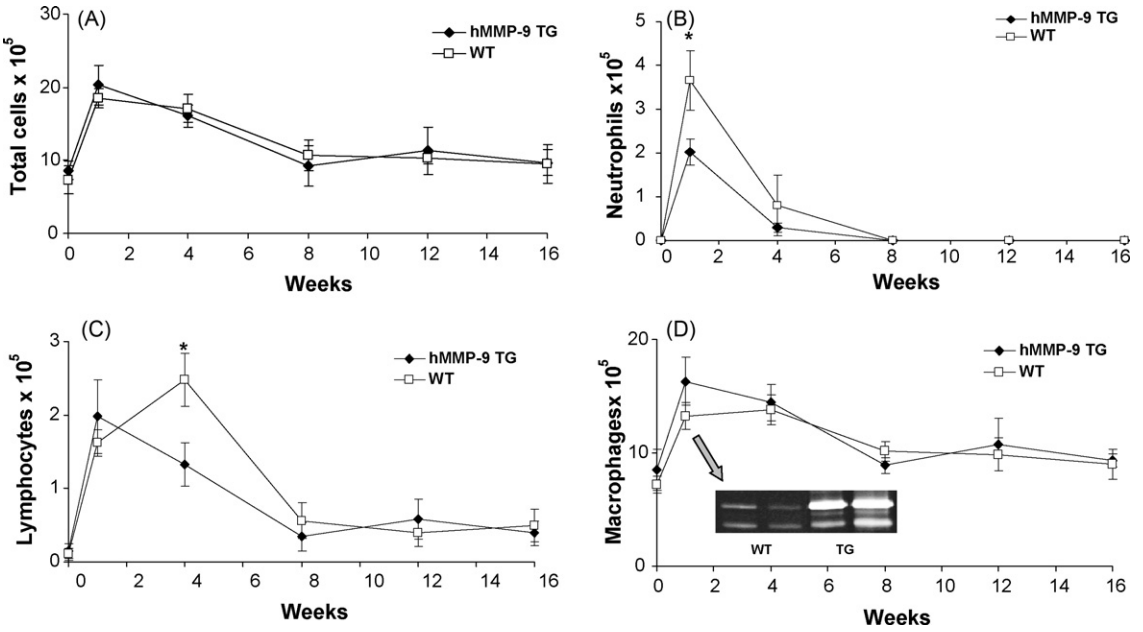

Fig. 2. Total and differential cell counts in BAL fluid from hMMP-9 TG and WT mice after bleomycin or saline instillation. (A) Total cell counts, (B) neutrophils, (C) lymphocytes, (D) macrophages. Inset in panel D shows gelatin zymogram from BAL cells of WT and hMMP9 TG mice at 7 days post-bleomycin. Results are shown as mean ± S.D. ($n = 6$). *$p < 0.05$, comparison of hMMP-9 TG with WT mice.

hMMP9 TG and WT mice (Fig. 4B and E). Inflammation consisted of both polymorphonuclear and mononuclear cells. At 4 weeks after bleomycin instillation, focal areas of fibrosis were observed in both hMMP9 TG and WT mice without any observable differences. However, more extensive and severe fibrosis developed in the WT mice at 8 weeks after bleomycin instillation. The deposition of collagen at this time point, as visualized by Masson's trichrome staining, was clearly more pronounced in the WT mice as compared to the staining in the hMMP9 TG mice (Fig. 4C and F). At 12 and 16 weeks after bleomycin, the extent of the lesions decreased in both groups and large areas of normal lung were observed. Small subpleural and peribronchiolar fibrotic foci persisted in a subset of animals from both groups of mice, at this stage. Semi-quantitative analysis of the histopathological changes demonstrated that the extent of lesion was higher in WT mice at 4 and 8 weeks after bleomycin instillation and the severity of the lesions and the percent of fibrosis were stronger at 8 weeks post-bleomycin compared to hMM9 TG mice (Table 2).

3.5. OH-proline content

Lung collagen was evaluated by measuring hydroxyproline content in the left lung. Similar basal levels of hydroxyproline were found in hMMP9 TG and WT mice (59 ± 2.1 μg/lung versus 61.1 ± 4.8 μg/lung). There was an age effect on hydroxyproline concen-

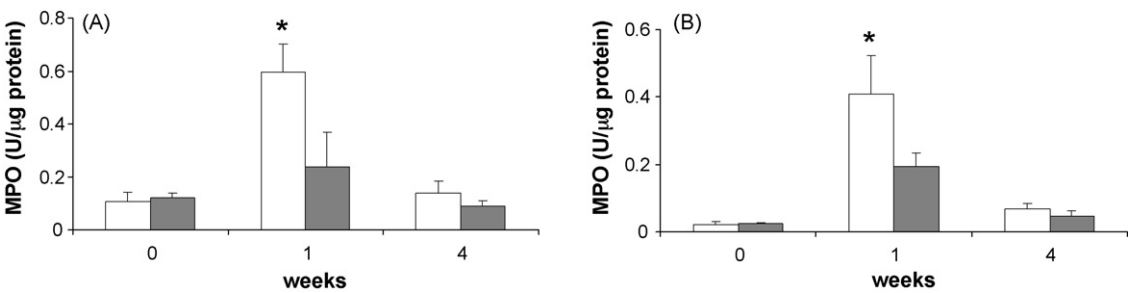

Fig. 3. Lung tissue and BAL myeloperoxidase activity in hMMP9 TG and WT mice. MPO activity was determined in lung tissue (A) and BAL fluids (B). Results are expressed as units/mg of protein and shown as mean ± S.D. ($n = 6$). *$p < 0.05$, comparison of hMMP-9 TG (gray bars) with WT mice (white bars).

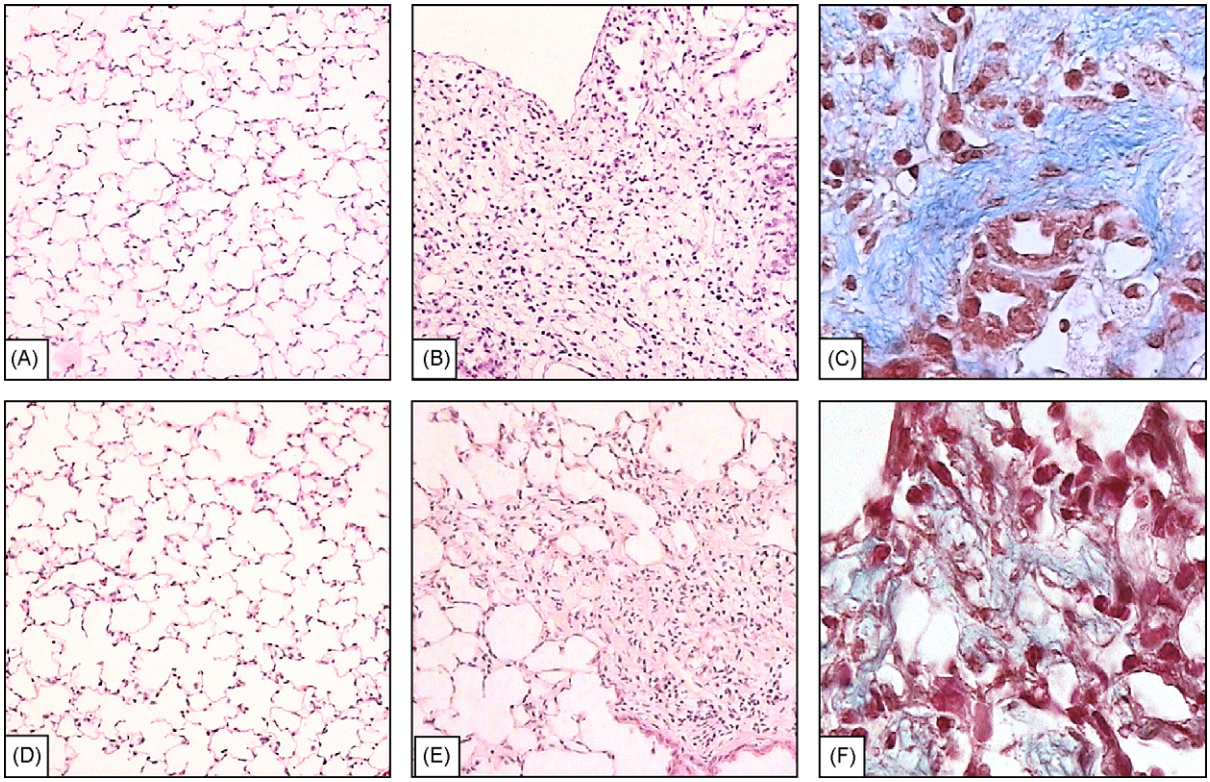

Fig. 4. Light micrographs of lung sections from hMMP9 TG and WT mice. Panels A and D illustrate WT and hMMP-9 TG control mice (hematoxylin and eosin, original magnification 10×). Panels B and E show WT and hMMP-9 TG mice at 8 weeks after bleomycin (hematoxylin and eosin, original magnification 10×). Panels C and F illustrate WT and hMMP-9 TG mice at 8 weeks after bleomycin (Masson trichrome; 40X).

tration, that was independent of treatment ($p = 0.69$ by likelihood ratio test). However, there were no significant differences across the time course for each genotype (data not shown).

Table 2
Semi-quantitative score of the morphological lesions

	Extent	Severity	Percentage of fibrosis
4 weeks			
WT	35 ± 21*	1.7 ± 0.5	25 ± 12
hMMP9 TG	19 ± 18	1.4 ± 0.5	21 ± 8
8 weeks			
WT	45 ± 16*	2.5 ± 0.5*	31 ± 18*
hMMP9 TG	21 ± 13	1.7 ± 0.5	23 ± 7
12 weeks			
WT	19 ± 20	1.1 ± 0.9	28 ± 24
hMMP9 TG	10 ± 9	1.2 ± 0.9	27 ± 23
16 weeks			
WT	10 ± 16	1.1 ± 0.9	6 ± 7
hMMP9 TG	5 ± 7	0.7 ± 0.8	5 ± 8

Results are shown as mean ± S.D. ($n = 6$–10).
* $p < 0.05$.

The effect of bleomycin instillation on the collagen content in WT mice paralleled the morphological findings. A significant augmentation was observed at 4 weeks post-bleomycin, reaching a three fold increase from baseline at 8 weeks (Fig. 5A and C). The effect of bleomycin treatment was found to differ significantly in the TG mice compared to the WT mice ($p < 0.001$ by likelihood ratio test). As illustrated in Fig. 5C, at 8 weeks after bleomycin instillation, OH-proline levels in WT mice were significantly higher compared with the hMMP9 TG mice (176.2 ± 20.4 versus 98.1 ± 15.4; $p < 0.01$). Hydroxyproline levels in hMMP9 TG mice never reached the hydroxyproline levels of WT mice (Fig. 5B and C). At 12 and 16 weeks post-bleomycin results were heterogeneous. In some mice hydroxyproline levels remained high, but in the majority of animals the content diminished showing no statistical difference with basal levels (Fig. 5A and B).

3.6. BALF cytokine profile

To explore possible mechanisms related to the decreased fibrotic response of the hMMP9 TG mice,

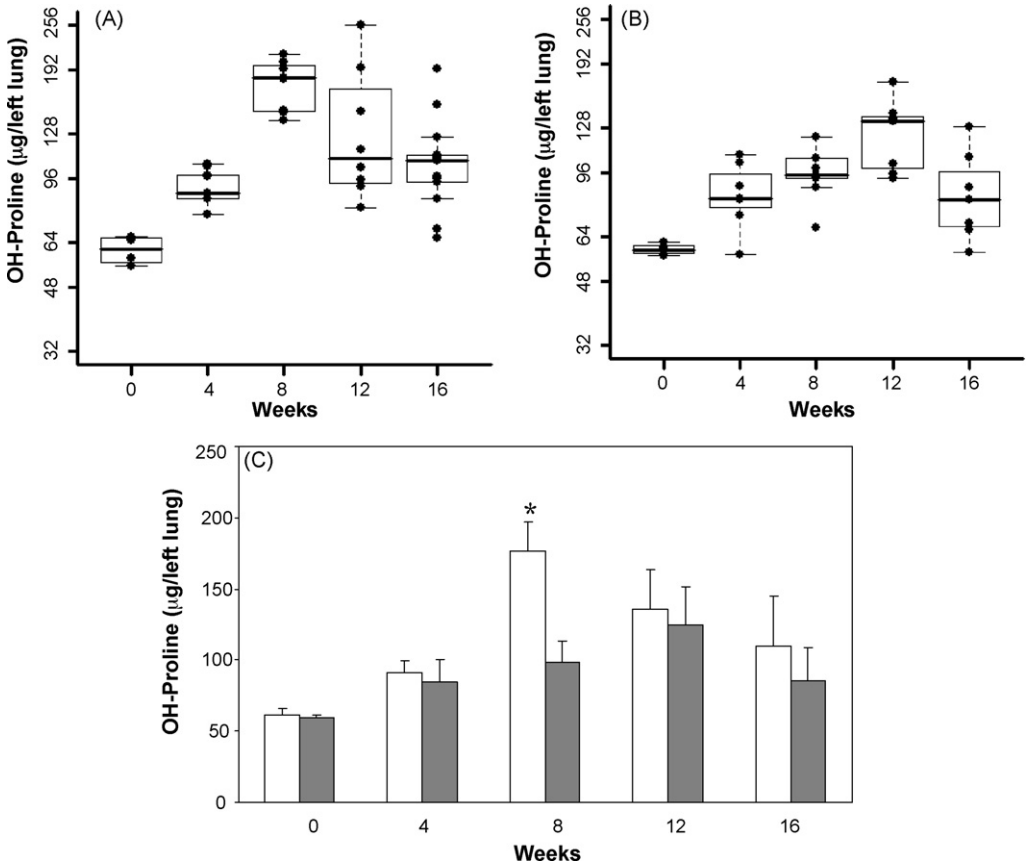

Fig. 5. Effect of bleomycin instillation on lung hydroxyproline. Boxplots of lung hydroxyproline content from WT mice (A) and hMMP-9 TG mice (B). Linear regression with log-transformed hydroxyproline concentration as response variable was used to analyze effects of treatment. Likelihood ratio testing was used to compute p-values. Results are shown as mean ± S.D. ($n = 8$–10). (C) Comparison of lung hydroxyproline content from WT (white bars) and hMMP-9 TG mice (gray bars); *$p < 0.01$.

we compared the levels of a variety of mouse cytokines implicated in lung inflammation and fibrosis, i.e., CRG-2, GM-SCF, IGFBP-3, IGFBP-5, IL-1b, KC, PF-4, SDF-1, TIMP-1 and TNF-α. Measurements were performed in BAL fluids obtained from hMMP9 TG and WT mice 1 and 4 weeks after bleomycin or saline intratracheal administration.

Representative examples of the membrane antibody arrays are shown in Fig. 6A. In WT mice, the level of IGFBP-3 was significantly higher at 1 and 4 weeks after bleomycin instillation compared with WT mice that received saline ($p < 0.01$). In hMMP9 TG mice IGFBP-3 was significantly increased only at the 1st week compared with controls ($p < 0.05$). However, at 1 week post-bleomycin administration, IGFBP-3 levels in hMMP9 TG mice were significantly lower than the levels found in the WT mice ($p < 0.01$) (Fig. 6B).

Differences in TIMP-1 levels were also detected between WT and TG mice post-bleomycin. Thus, in WT mice, the level of this MMP inhibitor was significantly increased at 1 and 4 weeks after bleomycin compared with controls ($p < 0.01$). By contrast, no significant difference in TIMP-1 levels was observed between bleomycin and saline-treated hMMP9 TG mice. At 1 week post-bleomycin TIMP1 was significantly increased in WT mice compared with hMMP9 TG mice ($p < 0.05$) (Fig. 6C). No differences were found in the other cytokines/chemokines evaluated.

We next explored the IGFBP-3 mRNA expression in control and bleomycin-treated WT and hMMP9 TG mice by quantitative real-time PCR. The levels of IGFBP-3 mRNA significantly increased after 1 and 4 weeks post-bleomycin in both WT and hMMP9 TG mice ($p < 0.05$). No significant differences were found between WT and hMMP9 TG mice at any time point (Fig. 7A).

3.7. MMP9 cleaves IGFBP-3

Since hMMP9 TG mice express similar gene levels of IGFBP-3, but showed a reduction of the lung lev-

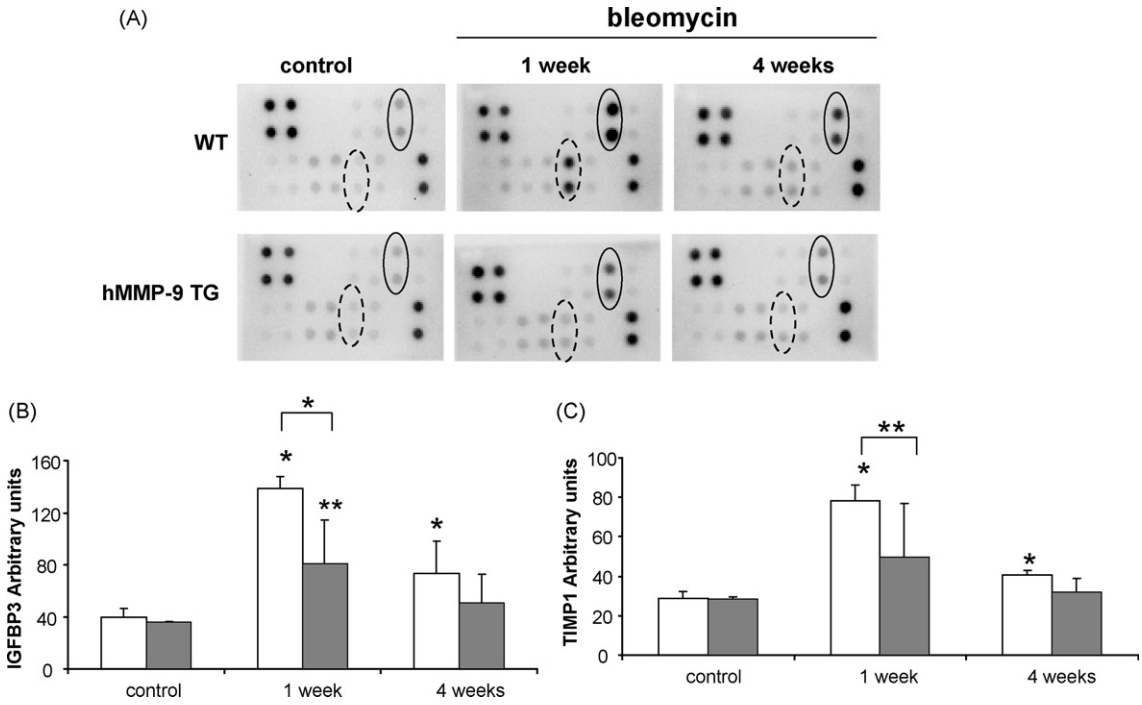

Fig. 6. Mouse protein-array analysis from BAL of hMMP9 TG and WT mice. (A) Representative mouse protein array showing the levels of CXCL10, GM-CSF, IGFBP-3, IGFBP-5, IL-1β, KC, PF-4, SDF-1, TIMP-1, and TNF-α from control, and from 1 and 4 weeks bleomycin-treated hMMP-9 TG and WT mice. IGFBP-3 is shown in closed ellipses, and TIMP1 in dotted ellipses. Positive controls are located in the upper left-hand corner and lower right-hand corner of each membrane. Negative controls are next to the four positive control spots. Panels B and C show densitometric analysis of IGFBP-3 (B) and TIMP-1 (C). Results are shown as means ± S.D. ($n = 6$). WT mice (white bars) and hMMP-9 TG (gray bars); $^{**}p < 0.01$, $^{*}p < 0.05$.

els of the protein we evaluated the effect of hMMP9 on IGFBP-3 *in vitro*. Western blot analysis showed that the intact mouse IGFBP-3 was represented by multiple glycosylated forms migrating at approximately 40–50 kDa molecular mass and a core protein form of 29 kDa (Fig. 7B, lane 1). Human MMP9 degraded mouse IGFBP-3 into a variety of lower molecular mass fragments (∼24 to 7 kDa) (Fig. 7B, lane 2). Additionally, two different mIGFBP-3 fragments of ∼18 and 12 kDa were observed when hMMP9 was activated with APMA (Fig. 7B, lane 3). The digestion of intact mIGFBP-3 was inhibited by 10 mM EDTA (Fig. 7B, lane 4).

3.8. IGFBP-3 substrate zymography

To test whether lungs from hMMP9 TG and WT mice contained proteases able to cleave IGFBP-3, BAL fluids obtained at 1 week after bleomycin instillation were examined by IGFBP-3 substrate zymography that included gel transfer of proteolytic fragments of IGFBP-3 and subsequent immunoblot. Results revealed immunoreactive bands corresponding to the molecular mass of human pro-MMP9 in BAL fluids from TG mice (Fig. 7C, lines 3 and 4). These immunoreactive bands disappeared when 10 mM EDTA was added to the incubation buffer, suggesting that mIGFBP-3 degradation was MMP dependent (data not shown).

3.9. Immunohistochemical localization of IGFBP3

Normal lungs from both WT and hMMP9 TG mice showed occasional staining in alveolar macrophages and around blood vessels (Fig. 8A and C). Immunoreactive IGFBP-3 protein localized in macrophages (Fig. 8B, inset) and in extracellular matrix in bleomycin-exposed animals, and it was clearly less abundant in the lungs from hMMP9 TG mice as compared to WT mice at 1 at 4 weeks as exemplified for 1 week in Fig. 8B and D.

4. Discussion

In the present study we analyzed the effect of the overexpression of MMP9 a metalloprotease mediating diverse biological functions on bleomycin induced pulmonary fibrosis. Following the model for 4 months, we demonstrated that overexpression of MMP9 in

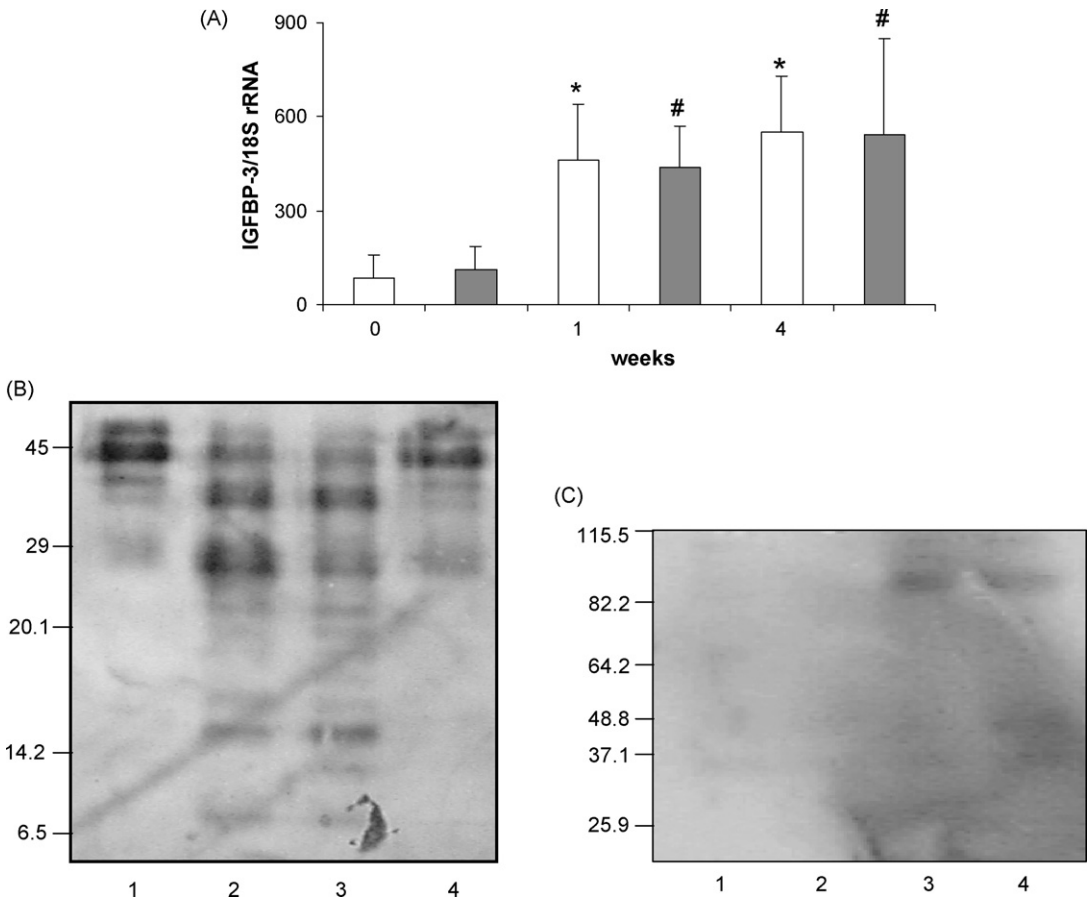

Fig. 7. Quantitative real-time PCR for IGFBP-3 and effect of MMP-9 on IGFBP-3. (A) IGFBP-3 mRNA level was determined by quantitative real-time PCR in lung tissue from hMMP-9 TG (gray bars) and WT (white bars), control and bleomycin-treated mice and normalized for 18S rRNA. Results are shown as means ± S.D. ($n = 6$). * and $^{\#}p < 0.05$ compared with their respective controls. (B) Western blot showing IGFBP-3 cleavage by MMP9. Lane 1: recombinant mouse IGFBP-3; lane 2: IGFBP-3 incubated with human MMP-9, lane 3: IGFBP-3 ± MMP-9 ± 1.5 mM APMA; lane 4: IGFBP-3 ± MMP-9 ± 100 mM EDTA. (C) IGFBP-3 substrate zymography. BAL fluids from 1 week after bleomycin instillation of WT (lanes 1 and 2) and hMMP-9 TG mice (lanes 3 and 4) were analyzed by IGFBP-3 substrate zymography and followed by gel transfer and immunoblot for IGFBP3 as described in Section 2. The bands indicate IGFBP-3-degrading proteinase activity in the BAL fluid of hMMP-9 TG mice.

macrophages induces a retarded and diminished lung fibrotic reaction. This effect was preceded by a decrease in neutrophil infiltration at 1 week, and decreased lymphocytes at 1 month post-bleomycin treatment. Interestingly, a lower level of IGFBP3 and TIMP1 was noticed in the transgenic mice compared to wild-type mice. To better understand the potential antifibrotic role of MMP9 we studied its' effect on IGFBP3, showing that MMP9 induced IGFBP3 cleavage.

MMP9 gene and protein expression has been found to be upregulated in IPF tissues (Selman et al., 2006, 2000; Zuo et al., 2002). Immunolocalization has identified MMP9 in a diversity of cell types in fibrotic lungs, including resident cells as alveolar type II cells, fibroblasts, and smooth muscle cells, and inflammatory cells (neutrophils and macrophages) (Fukuda et al., 1998; Hayashi et al., 1996; Lemjabbar et al., 1999; Pérez-Ramos et al., 1999; Selman et al., 2000).

As MMP9 cleaves type IV collagen, its role has been largely associated with cell migration across or through basement membranes. This concept has been supported by studies demonstrating that migration of basal cells after tracheal wounding is dependent on MMP9 activation and by experiments in MMP9 deficient mice revealing minimal alveolar bronchiolization after bleomycin (Betsuyaku et al., 2000; Legrand et al., 1999).

MMP9, however, is a multifunctional enzyme that participates in a large variety of physiological pathways and to deduce the consequences of its expression/activation *in vivo* only by its ability to degrade basement membranes is too simplistic. Apart from

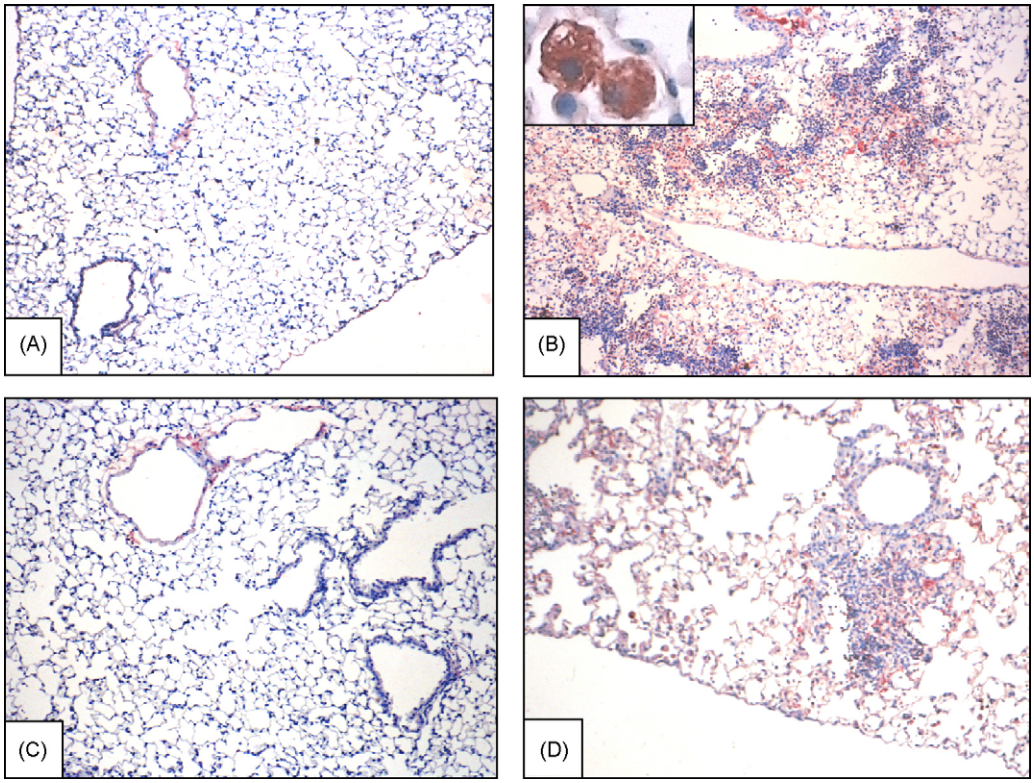

Fig. 8. Immunolocalization of IGFBP-3 in hMMP9 TG and WT lungs. Immunoreactive IGFBP-3 protein was revealed with 3-amino-9-ethylcarbazole and lung tissue samples were counterstained with hematoxylin. Panels (A and C) Lung specimens from WT and hMMP-9 TG control mice. Panels (B and D) IGFBP-3 staining in WT and hMMP-9 TG mice after 1 week bleomycin exposure (10× original magnification). Inset in panel B shows stained alveolar macrophages (40×).

digesting components of the ECM, such as collagens type IV, V, XIV, decorin, gelatin, laminin, aggrecan, elastin, versican, vitronectin, and osteonectin, MMP9 activates other MMPs including pro-MMP2, pro-MMP9, and pro-MMP13. Additionally, MMP9 modulates the activity of several cytokines including IL-1 β, IP-10/CXCL10, IL-2Rα, pro-IL-8, monokine induced by interferon (IFN)-gamma (MIG), granulocyte chemotactic protein-2 (GCP-2), pro-TNF-α, epithelial neutrophil-activating protein (ENA-78), pro-transforming growth factor beta (TGF-β), tumstatin, IFN-β, fibroblast growth factor receptor-1 (FGFR-1), endostatin, connective tissue-activating peptide III (CTAP-III), plasminogen, SDF-1, α1-proteinase inhibitor, growth-related gene alpha (GROα), α2-macroglobulin, and KiSS-1/metastin (Atkinson & Senior, 2003; Folgueras, Pendas, Sanchez, & Lopez-Otin, 2004; Pardo & Selman, 2006; Schonbeck, Mach, & Libby, 1998; Van den Steen, Proost, Wuyts, Van Damme, & Opdenakker, 2000; Van den Steen et al., 2003).

In this context, the numerous potential substrates of MMP9 and the variety of cell types expressing this enzyme enlarge the possibilities of its involvement in multiple events as the proteolytic executor and regulator of processes occurring in the lung microenvironment during the development of pulmonary fibrosis.

It has been demonstrated that MMP9 may play a dual role in the migration of inflammatory cells to sites of injury. Regarding neutrophil infiltration, it has been shown that MMP9 processes IL-8, a potent human neutrophil chemokine, into a more active mediator. In the mouse, where there is no close homologue to IL-8, gelatinase B cleaves mouse GCP-2/LIX, a potent mouse CXC chemokine also potentiating its biological activity (Van den Steen et al., 2000, 2003). On the other hand however, MMP9 also degrades neutrophilic chemokines like GROα, CTAP-III, and PF-4 (Van den Steen et al., 2000, 2003). In this context, MMP9 has been associated with a prominent inhibitory effect on BAL leukocyte accumulation and neutrophilia in IL-13-induced inflammation and remodeling (Lanone et al., 2002).

Our transgenic mice overexpressing MMP9 exhibited reduced accumulation of neutrophils after bleomycin treatment supporting the last findings (Fig. 9). Impor-

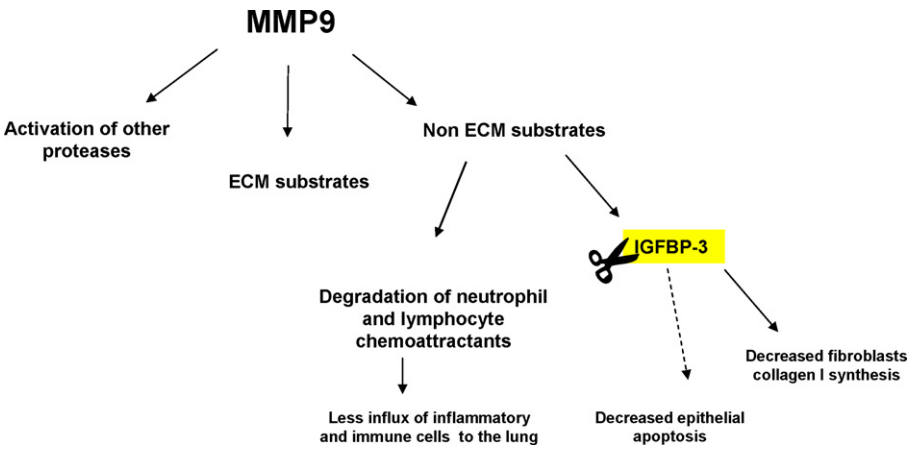

Fig. 9. Possible involvement of MMP9 in the lung microenvironment. Excess of MMP9 degrades insulin growth factor binding protein-3 resulting in a reduction of the fibrotic response. Also, breakdown of some chemokines may reduce the inflammatory response.

tantly, regarding the relationship between neutrophils and experimental fibrosis, several studies have demonstrated the relevance of an early neutrophilic response in the development of lung fibrosis. Less neutrophils in the BAL has been associated with less lung fibrosis in mice deficient in gamma-glutamyl transpeptidase (Pardo et al., 2003), as well as in mice deficient in MMP7 (Li, Park, Wilson, & Parks, 2002; Zuo et al., 2002).

Also, biphasic regulation of MMP9 has been reported regarding the putative regulation of IL-1β activity at sites of acute or chronic inflammation. Thus, MMP9 quickly converts the inactive pIL-1β into a biologically active form, but upon prolonged exposure, further degrades IL-1β, yielding loss of biologic activity (Schonbeck et al., 1998).

Another important finding in our study was the difference in TIMP1 expression between hMMP9 TG and WT mice after bleomycin. Thus, whereas a vigorous increase of TIMP1 was observed in the lungs of the wild-type mice at 1 and 4 weeks post-instillation, a modest tendency to increase was noticed in the transgenic mice at 1 week. TIMP1 is an important endogenous inhibitor of most MMPs that is usually overexpressed in experimental models of lung fibrosis including bleomycin instillation, paraquat plus hyperoxia, and adenoviral gene models transfer of active transforming growth factor (Swiderski, Dencoff, Floerchinger, Shapiro, & Hunninghake, 1998) as well as in IPF (Garcia-Alvarez et al., 2006; Hayashi et al., 1996; Selman et al., 2000). Moreover, mice susceptible and resistant to lung fibrosis differ in the TIMP1 response to injury (Kolb et al., 2002). Therefore, these findings suggest that the difference in the fibrotic response between hMMP9 TG and WT mice may be at least partially related to the TIMP-1 expression. However, TIMP-1 deficient mice develop similar lung fibrosis compared with wild-type littermates when instilled with bleomycin suggesting that upregulation of TIMP-1 alone is not enough to explain collagen accumulation (Kim et al., 2005).

The reason for decreased TIMP1 in our model is presently unknown. However, it can be suggested that reduced TIMP1 may be at least partially related to excess MMP9 since this enzyme, besides interacting with the catalytic domain of the active form of TIMP-1, also forms a tight complex with TIMP-1 through the C-terminal domain with the hemopexin domain of proMMP9 (23). The reason for this dual association is unknown, except that proMMP9-TIMP complexes are potential inhibitors of metalloproteinases (Nagase et al., 2006).

Another interesting finding in our study was the diminished increase in insulin-like growth factor binding protein 3 in the BAL fluids and lungs of hMMP9 TG mice compared to wild-type mice after bleomycin instillation. IGFBPs are a family of IGF-binding proteins that have a high affinity for IGFs, preventing them from binding to their receptors and enhancing IGF-stimulated cell growth (Bonner & Brody, 1995; Jones & Clemmons, 1995). IGFBP3, in addition to its action as a carrier of IGFs, has been shown to inhibit growth and proliferation, and induce apoptosis in a variety of cell lines via IGF-independent mechanisms involving interactions with plasma, extracellular matrix and cell-surface molecules, and nuclear transport (Lee & Cohen, 2002; Singh, Charkowicz, & Mascarenhas, 2004).

It has been demonstrated that IGFBPs are involved in the regulation of synthesis and degradation of extracellular matrix. Important to our findings is that both IGFBP3

and -5 are secreted in excess by fibroblasts from IPF patients compared to fibroblasts from normal lungs, and that both augment fibroblast matrix production which may contribute to the fibrogenic process (Pilewski, Liu, Henry, Knauer, & Feghali-Bostwick, 2005). Also it has been reported that IGFBP3, -4, and -5 are increased in IPF lung tissues and in BAL obtained from patients with IPF (Aston et al., 1995; Pala et al., 2001; Pilewski et al., 2005; Selman et al., 2006;). IGFBP4 was observed in active bronchiolar basal epithelial cells while IGFBP3 and IGFBP5 in fibroblasts surrounding airspaces, and epithelial cells in bronchioles and alveoli (Pilewski et al., 2005; Selman et al., 2006). All this growing body of evidence indicates that several members of the IGFBP family may be involved in the fibrotic lung response. It could be hypothesized that the decreased lung fibrotic response of the transgenic mice overexpressing MMP9 associated with a decrease of the IGFBP3 may be related with reduced ECM synthesis by mesenchymal cells as well as a diminished epithelial cell apoptosis (Fig. 9).

A recent study has shown that mice exposed to adenovirus expressing human IGFBP-5 but not to IGFBP3 developed peribronchial, perivascular, and interstitial fibrosis (Yasuoka et al., 2006) suggesting that the likely profibrotic mechanisms of the IGFBPs may differ among them.

IGFBP3 cellular actions are modulated by post-translational events, including glycosylation, phosphorylation, and proteolysis. Specific proteases for IGFBP3 have been described, including serine proteases, cathepsins, and matrix metalloproteinases. IGFBPs degrading protease activities including MMP1, MMP3, MMP7, MMP9, MMP19, and ADAM 28 have been described in biological fluids and conditioned media from numerous cell lines. It has been shown that changes in IGFBP3 concentration, as a result of proteolytic cleavage may lead to alterations in IGFBP3-mediated mechanisms (Fowlkes et al., 1994; Hemers et al., 2005; Manes et al., 1999; Mochizuki, Shimoda, Shiomi, Fujii, & Okada, 2004; Sadowski, Dietrich, Koschinsky, & Sedlacek, 2003).

In this work, we showed evidence indicating that despite similar levels of gene expression IGFBP3 protein is decreased in the hMMP9 TG mice. Also we showed that human recombinant MMP9, and BAL MMP9 from the hMMP9 TG mice degrade IGFBP3 suggesting that the lower level of this mediator in the TG mouse might be attributed to the increased level of MMP9 and decreased levels of TIMP1.

In summary, our results provide a potential mechanism by which MMP9 secreted from macrophages can exert an anti-fibrotic effect through the reduction of potential profibrotic mediators, such as TIMP-1 and IGFBP-3.

These findings together with those that have suggested a profibrotic role of this enzyme reveal the importance of MMP9 activity in promoting or attenuating the fibrotic response. An emerging hypothesis is that the cell type (neutrophils versus macrophages versus epithelial cells), the location of the activity (alveolar septum versus basement membrane), the target substrate(s) and the level of expression/activity of the enzyme (too little or too much) may turn on different pathways in response to injury. Understanding the mechanisms controlling the pattern of MMP9 expression/activity in the lung microenvironment will therefore help to clarify some of the processes leading to fibrosis.

Acknowledgements

This work was supported by a grant from CONACYT 41043-M and by Universidad Nacional Autonoma de Mexico SDI.PTID.05.6. S.C. was funded by CONACYT.

References

Aston, C., Jagirdar, J., Lee, T. C., Hur, T., Hintz, R. L., & Rom, W. N. (1995). Enhanced insulin-like growth factor molecules in idiopathic pulmonary fibrosis. *Am. J. Respir. Crit. Care Med.*, *151*, 1597–1603.

Atkinson, J. J., & Senior, R. M. (2003). Matrix metalloproteinase-9 in lung remodeling. *Am. J. Respir. Cell Mol. Biol.*, *28*, 12–24.

Betsuyaku, T., Fukuda, Y., Parks, W. C., Shipley, J. M., & Senior, R. M. (2000). Gelatinase B is required for alveolar bronchiolization after intratracheal bleomycin. *Am. J. Pathol.*, *157*, 525–535.

Bonner, J. C., & Brody, A. R. (1995). Cytokine-binding proteins in the lung. *Am. J. Physiol.*, *268*, L869–L878.

Cisneros-Lira, J., Gaxiola, M., Ramos, C., Selman, M., & Pardo, A. (2003). Cigarrete smoke exposure potentiates bleomycin-induced lung fibrosis in guinea pigs. *Am. J. Physiol. Lung Cell Mol. Physiol.*, *285*, L949–L956.

Folgueras, A. R., Pendas, A. M., Sanchez, L. M., & Lopez-Otin, C. (2004). Matrix metalloproteinases in cancer: From new functions to improved inhibition strategies. *Int. J. Dev. Biol.*, *48*, 411–424.

Fowlkes, J. L., Enghild, J. J., Suzuki, K., & Nagase, H. (1994). Matrix metalloproteinases degrade insulin-like growth factor-binding protein-3 in dermal fibroblast cultures. *J. Biol. Chem.*, *269*, 25742–32574.

Fukuda, Y., Ishizaki, M., Kudoh, S., Kitaichi, M., & Yamanaka N. (1998). Localization of matrix metalloproteinases-1, -2, and -9 and tissue inhibitor of metalloproteinase-2 in interstitial lung diseases. *Lab. Invest.*, *78*, 687–698.

Garcia-Alvarez, J., Ramirez, R., Checa, M., Nuttall, R. K., Sampieri, C. L., Edwards, D. R., et al. (2006). Tissue inhibitor of metalloproteinase-3 is up-regulated by transforming growth factor-beta1 *in vitro* and expressed in fibroblastic foci *in vivo* in idiopathic pulmonary fibrosis. *Exp. Lung Res.*, *32*, 201–214.

Hayashi, T., Stetler-Stevenson, W. G., Fleming, M. V., Fishback, N., Koss, M. N., Liotta, L. A., et al. (1996). Immunohistochemical

study of metalloproteinases and their tissue inhibitors in the lungs of patients with diffuse alveolar damage and idiopathic pulmonary fibrosis. *Am. J. Pathol.*, *149*, 1241–1256.

Hemers, E., Duval, C., McCaig, C., Handley, M., Dockray, G. J., & Varro, A. (2005). Insulin-like growth factor binding protein-5 is a target of matrix metalloproteinase-7: Implications for epithelial-mesenchymal signaling. *Cancer Res.*, *65*, 7363–7369.

Jones, J. I., & Clemmons, D. R. (1995). Insulin-like growth factors and their binding proteins: Biological actions. *Endocrinol. Rev.*, *16*, 3–34.

Kim, K. H., Burkhart, K., Chen, P., Frevert, C. W., Randolph-Habecker, J., Hackman, R. C., et al. (2005). Tissue inhibitor of metalloproteinase-1 deficiency amplifies acute lung injury in bleomycin-exposed mice. *Am. J. Respir. Cell Mol. Biol.*, *33*, 271–279.

Kolb, M., Bonniaud, P., Galt, T., Sime, P. J., Kelly, M. M., Margetts, P. J., et al. (2002). Differences in the fibrogenic response after transfer of active transforming growth factor-beta1 gene to lungs of "fibrosis-prone" and "fibrosis-resistant" mouse strains. *Am. J. Respir. Cell Mol. Biol.*, *27*, 141–150.

Lanone, S., Zheng, T., Zhu, Z., Liu, W., Lee, C. G., Ma, B., et al. (2002). Overlapping and enzyme-specific contributions of matrix metalloproteinases-9 and -12 in IL-13-induced inflammation and remodeling. *J. Clin. Invest.*, *110*, 463–474.

Lee, K. W., & Cohen, P. (2002). Nuclear effects: Unexpected intracellular actions of insulin-like growth factor binding protein-3. *J. Endocrinol.*, *175*, 33–40.

Legrand, C., Gilles, C., Zahm, J. M., Polette, M., Buisson, A. C., Kaplan, H., et al. (1999). Airway epithelial cell migration dynamics: MMP-9 role in cell-extracellular matrix remodeling. *J. Cell Biol.*, *146*, 517–529.

Lemaitre, V., O'Byrne, T. K., Borczuk, A. C., Okada, Y., Tall, A. R., & D'Armiento, J. (2001). ApoE knockout mice expressing human matrix metalloproteinase-1 in macrophages have less advanced atherosclerosis. *J. Clin. Invest.*, *107*, 1227–1234.

Lemaitre, V., O'Byrne, T. K., Dalal, S. S., Tall, A. R., & D'Armiento, J. M. (1999). Macrophage-specific expression of human collagenase (MMP-1) in transgenic mice. *Ann. N.Y. Acad. Sci.*, *878*, 736–739.

Lemjabbar, H., Gosset, P., Lechapt-Zalcman, E., Franco-Montoya, M. L., Wallaert, B., Harf, A., et al. (1999). Overexpression of alveolar macrophage gelatinase B (MMP-9) in patients with idiopathic pulmonary fibrosis: Effects of steroid and immunosuppressive treatment. *Am. J. Respir. Cell Mol. Biol.*, *20*, 903–913.

Li, Q., Park, P. W., Wilson, C. L., & Parks, W. C. (2002). Matrilysin shedding of syndecan-1 regulates chemokine mobilization and transepithelial efflux of neutrophils in acute lung injury. *Cell*, *111*, 635–646.

Manes, S., Llorente, M., Lacalle, R. A., Gomez-Mouton, C., Kremer, L., Mira, E., et al. (1999). The matrix metalloproteinase-9 regulates the insulin-like growth factor-triggered autocrine response in DU-145 carcinoma cells. *J. Biol. Chem.*, *274*, 6935–6945.

Mochizuki, S., Shimoda, M., Shiomi, T., Fujii, Y., & Okada, Y. (2004). ADAM28 is activated by MMP-7 (matrilysin-1) and cleaves insulin-like growth factor binding protein-3. *Biochem. Biophys. Res. Commun.*, *315*, 79–84.

Nagase, H., Visse, R., & Murphy G. (2006). Structure and function of matrix metalloproteinases and TIMPs. *Cardiovasc. Res.*, *69*, 562–573.

Pala, L., Giannini, S., Rosi, E., Cresci, B., Scano, G., Mohan, S., et al. (2001). Direct measurement of IGF-I and IGFBP-3 in bronchoalveolar lavage fluid from idiopathic pulmonary fibrosis. *J. Endocrinol. Invest.*, *24*, 856–864.

Pardo, A., Barrios, R., Gaxiola, M., Segura-Valdez, L., Carrillo, G., Estrada, A., et al. (2000). Increase of lung neutrophils and upregulation of neutrophil gelatinase B and collagenase in hypersensitivity pneumonitis. *Am. J. Respir. Crit. Care Med.*, *161*, 1698–1704.

Pardo, A., Ruiz, V., Arreola, J. L., Ramírez, R., Cisneros-Lira, J., Gaxiola, M., et al. (2003). Bleomycin-induced pulmonary fibrosis is attenuated in gamma glutamyl transpeptidase-deficient mice. *Am. J. Respir. Crit. Care Med.*, *167*, 925–932.

Pardo, A., & Selman M. (2002). Molecular mechanisms of pulmonary fibrosis. *Front. Biosci.*, *7*, d1743–d1761.

Pardo, A., & Selman M. (2006). Matrix metalloproteases in the aberrant fibrotic tissue remodeling. *Proc. Am. Thorac. Soc.*, *3*, 383–388.

Pérez-Ramos, J., Segura, L., Ramírez, R., Vanda, B., Selman, M., & Pardo, A. (1999). Matrix metalloproteinases 2,9 and 13 and tissue inhibitor of metalloproteinases 1 and 2 in early and late lesions of experimental lung silicosis. *Am. J. Respir. Crit. Care Med.*, *160*, 1274–1282.

Pilewski, J. M., Liu, L., Henry, A. C., Knauer, A. V., & Feghali-Bostwick, C. A. (2005). Insulin-like growth factor binding proteins 3 and 5 are overexpressed in idiopathic pulmonary fibrosis and contribute to extracellular matrix deposition. *Am. J. Pathol.*, *166*, 399–407.

Ruiz, V., Ordonez, R. M., Berumen, J., Ramirez, R., Uhal, B., Becerril, C., et al. (2003). Unbalanced collagenase/TIMP-1 expression and epithelial apoptosis in experimental lung fibrosis. *Am. J. Physiol. Lung Cell Mol. Physiol.*, *285*, L1026–L1036.

Sadowski, T., Dietrich, S., Koschinsky, F., & Sedlacek, R. (2003). Matrix metalloproteinase 19 regulates insulin-like growth factor-mediated proliferation, migration, and adhesion in human keratinocytes through proteolysis of insulin-like growth factor binding protein-3. *Mol. Biol. Cell*, *14*, 4569–4580.

Schonbeck, U., Mach, F., & Libby, P. (1998). Generation of biologically active IL-1b by matrix metalloproteinases: A novel caspase-1-independent pathway of IL-1b processing. *J. Immunol.*, *161*, 3340–3346.

Selman, M., Pardo, A., Barrera, L., Estrada, A., Watson, S. R., Wilson, K., et al. (2006). Gene expression profiles distinguish idiopathic pulmonary fibrosis from hypersensitivity pneumonitis. *Am. J. Respir. Crit. Care Med.*, *173*, 188–198.

Selman, M., Ruiz, V., Cabrera, S., Segura, L., Ramírez, R., Barrios, R., et al. (2000). TIMP -1, -2,-3 and -4 in idiopathic pulmonary fibrosis. A prevailing non degradative lung microenvironment? *Am. J. Physiol.*, *279*, L562–L574.

Singh, B., Charkowicz, D., & Mascarenhas, D. (2004). Insulin-like growth factor-independent effects mediated by a C-terminal metal-binding domain of insulin-like growth factor binding protein-3. *J. Biol. Chem.*, *279*, 477–487.

Suga, M., Iyonaga, K., Okamoto, T., Gushima, Y., Miyakawa, H., Akaike, T., et al. (2000). Characteristic elevation of matrix metalloproteinase activity in idiopathic interstitial pneumonias. *Am. J. Respir. Crit. Care Med.*, *162*, 1949–1956.

Swiderski, R. E., Dencoff, J. E., Floerchinger, C. S., Shapiro, S. D., & Hunninghake, G. W. (1998). Differential expression of extracellular matrix remodeling genes in a murine model of bleomycin-induced pulmonary fibrosis. *Am. J. Pathol.*, *152*, 821–828.

Van den Steen, P. E., Proost, P., Wuyts, A., Van Damme, J., & Opdenakker, G. (2000). Neutrophil gelatinase B potentiates interleukin-8 tenfold by aminoterminal processing, whereas it degrades CTAP-III, PF-4, and GRO- and leaves RANTES and MCP-2 intact. *Blood*, *96*, 2673–2681.

Van den Steen, P. E., Wuyts, A., Husson, S. J., Proost, P., Van Damme, J., & Opdenakker, G. (2003). Gelatinase B/MMP-9 and neutrophil collagenase/MMP-8 process the chemokines human GCP-2/CXCL6, ENA-78/CXCL5 and mouse GCP-2/LIX and modulate their physiological activities. *Eur. J. Biochem.*, *270*, 3739–3749.

Woessner, J. F. (1961). The determination of hydroxyproline in tissue and protein samples containing small proportions of this amino acid. *Arch. Biochem. Biophys.*, *93*, 440–447.

Yaguchi, T., Fukuda, Y., Ishizaki, M., & Yamanaka, N. (1998). Immunohistochemical and gelatin zymography studies for matrix metalloproteinases in bleomycin-induced pulmonary fibrosis. *Pathol. Int.*, *48*, 954–963.

Yasuoka, H., Zhou, Z., Pilewski, J. M., Oury, T. D., Choi, A. M., & Feghali-Bostwick, C. A. (2006). Insulin-like growth factor-binding protein-5 induces pulmonary fibrosis and triggers mononuclear cellular infiltration. *Am. J. Pathol.*, *169*, 1633–1642.

Zuo, F., Kaminski, N., Eugui, E., Allard, J., Yakhini, Z., Ben-Dor, A., et al. (2002). Gene expression analysis reveals matrilysin as a key regulator of pulmonary fibrosis in mice and humans. *Proc. Natl. Acad. Sci. U.S.A.*, *99*, 6292–6297.